molecular pharmaceutics

Article

Cite This: *Mol. Pharmaceutics* 2018, 15, 1664−1673

Computer-Aided Formulation Design for a Highly Soluble Lutein−Cyclodextrin Multiple-Component Delivery System

Qianqian Zhao,[†] Nikhila Miriyala,[‡] Yan Su,[†] Weijie Chen,[†] Xuejiao Gao,[†] Ling Shao,[†] Ru Yan,[†] Haifeng Li,[§] Xiaojun Yao,[∥] Dongsheng Cao,[⊥] Yitao Wang,[†] and Defang Ouyang*[,†]

[†]State Key Laboratory of Quality Research in Chinese Medicine, Institute of Chinese Medical Sciences (ICMS), University of Macau, Macau, China

[‡]Aston Pharmacy School, School of Life and Health Sciences, Aston University, Birmingham B4 7ET, United Kingdom

[§]Institute of Applied Physics and Materials Engineering, University of Macau, Macau, China

[∥]State Key Laboratory of Quality Research in Chinese Medicine, Macau Institute for Applied Research in Medicine and Health, Macau University of Science and Technology, Macau, China

[⊥]School of Pharmaceutical Science, Central South University, Changsha 410013, P. R. China

ABSTRACT: Cyclodextrin (CD) complexation is widely used for the solubilization of poorly soluble drugs in the pharmaceutical industry. Current research was to develop a highly soluble lutein−cyclodextrin multiple-component delivery system (lutein−CD-MCDS) by combined modeling and experimental approaches. Both phase solubility diagram and molecular dynamics (MD) simulation results revealed that the interactions between lutein and CDs were very weak, which confirmed the insignificant solubility improvement of lutein−CD binary system. On the basis of theoretical calculation and preliminary CD studies, lutein−CD-MCDS was developed with over 400-fold solubility improvement after formulation screening. MD simulation indicated that the auxiliary polymers of TWEEN 80 and poloxamer 188 in the lutein−CD-MCDS introduced bridged interaction between lutein and γ-CD to increase the solubility, dissolution rate, and stability of the complex. The lutein−CD-MCDS was characterized by *in vitro* dissolution test, differential scanning colorimetry (DSC), Fourier transform infrared spectroscopy (FT-IR), scanning electron microscopy (SEM), and powder X-ray diffraction (PXRD). Moreover, lutein−CD-MCDS had significantly higher uptake in Caco-2 cells than free lutein. The relative bioavailability of the lutein−CD-MCDS increased to 6.6-fold compared to pure lutein, and to 1.2-fold compared with commercial lutein soft capsules. In conclusion, the highly soluble lutein−CD-MCDS with significant improvement in both the solubility and bioavailability was developed and characterized by combined modeling and experimental approaches. Our research indicates that computer-aided formulation design is a promising approach for future formulation development.

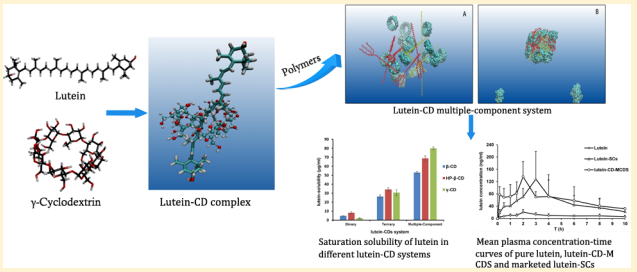

KEYWORDS: *lutein, cyclodextrin, multiple-component system, molecular dynamics simulation, bioavailability, computer-aided formulation design*

INTRODUCTION

Lutein, a kind of xanthophyllic carotenoid, naturally occurs in fruits and vegetables, which has been gaining attention lately because of its various physiological activities, including antioxidant, free radical scavenging, and anti-inflammation.[1−3] Lutein has the highest concentration in human retina, which is closely associated with its protective function against retina neural damage, age-related macular degeneration (AMD), and cataracts.[4,5] Although lutein is a vital macular pigment with many biological functions, dietary supplementation is the only source of lutein because human cannot synthesize it.[6] Like other carotenoids, lutein has a unique structure with nine conjugated double bonds in the polyene chain (Figure 1), which presents its high hydrophobicity and high sensitivity against light, heat, oxygen, and acid.[7] Naturally, there is the poor solubility and stability of lutein in digestive fluids, resulting in very limited intestinal absorption, bioavailability, and pharmaceutical application.[8] Recent findings demonstrated that the bioavailability of lutein strongly depended on the administration routes, delivery vehicles, and formulation.[8,9] Currently there were various formulation strategies to preserve lutein's chemical and physiological activities, as well as improve its solubility and bioavailability, such as suspension formulations, self-nanoemulsifying drug delivery systems, liposome, lipid particulate systems, and so on.[10−14] However, current formulation strategies did not achieve a satisfactory effect.

Received: January 18, 2018
Revised: March 2, 2018
Accepted: March 5, 2018
Published: March 5, 2018

DOI: 10.1021/acs.molpharmaceut.8b00056
Mol. Pharmaceutics 2018, 15, 1664−1673

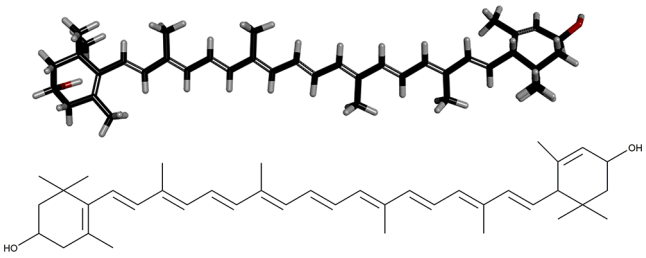

Figure 1. Chemical structure of lutein: (A) 2D structure; (B) 3D structure. Black bonds represent the carbon element, hydrogen element is in white, and oxygen element is in red.

Cyclodextrin (CD) complexation has been widely used for the delivery of poorly soluble lipophilic drugs.[15] CDs possess a round truncated-cone shape with a hydrophobic inner cavity and hydrophilic surface, which enable CDs to accommodate poorly water-soluble drugs into the inner cavity to form water-soluble drug−CD complexes.[16−18] The unique properties of CDs enable them to have the ability to enhance oral bioavailability and improve stability of drug candidates, which have made them attractive carriers for formulation development. For example, Nalawade and Gajjar demonstrated that spray-dried complexes of lutein with beta-cyclodextrin (β-CD) and its derivatives (e.g., hydroxypropyl beta-cyclodextrin (HP-β-CD) and methyl beta-cyclodextrin (Me-β-CD)) improved the solubility of lutein and its *in vitro* antiproliferative activity.[19] In addition to simply using CDs as a delivery vehicle, novel lipid nanoparticle with 2% HP-β-CD has been developed as a good delivery system to enhance lutein accumulation and partition in the cornea.[20]

Some drug candidates with big spatial structures and/or strong lipophilic characteristics have been reported to form CD complexes with weak binding constant,[17,21−23] which may result in drug precipitation in the gastrointestinal tract.[24,25] To overcome these bottlenecks, the third or fourth excipients, for examlple, surfactants, oils, waxes, polymers, and phospholipids, may be possessed in the formulation to form CD multiple-component systems.[26] Various CD multiple-component systems including drug/CD/polymers, drug/CD/liposomes, and drug/CD/ions have been studied for further enhancing the solubilization and complexation efficiency of CDs.[17] The auxiliary substances may interact with CDs to help to decrease drug crystallinity and to increase synergetic effects on the solubilizing action, which further improve the desired physicochemical and transport properties of the given drugs.[26,27] Thus, CD multiple-component systems can modulate *in vitro* and *in vivo* dissolution of drug−CD complexes, thereby contributing to the modification of the drug pharmacokinetic profile. Therefore, CD multiple-component systems have emerged as a promising drug delivery for poorly soluble drugs. However, formulation development of CD multiple-component systems is quite challenging for pharmaceutical scientists by trial-and-error in the laboratory. Moreover, it is difficult for traditional experimental approaches to reveal the molecular interactions in the multiple-component formulations.[28]

Molecular modeling methods, like docking, molecular dynamics (MD), and quantum mechanics (QM), can mimic the behavior of these systems at the atomistic level.[24,29] These modeling methods have been playing an important role to provide three-dimensional structures and to understand the mechanism of CD delivery systems, which greatly assist the formulation design and simplify the formulation screening procedures.[30,31] Our group previously investigated the molecular mechanism of ibuprofen−CD binary systems by three different molecular simulation approaches (docking, quantum mechanics, and molecular dynamics). Results from MD simulation showed good correlation with the results obtained through experimental methods.[32] In addition, the molecular interaction of etodolac−CD binary and ternary systems was investigated by the analysis of 3D structure, binding energy, and H-bond calculation, and the more stable complex formation with L-arginine was finally confirmed by both computational and experimental studies.[26]

This study aimed to design a highly soluble lutein−cyclodextrin multiple-component delivery system with the assistance of molecular modeling techniques, for the improvement of solubility, dissolution rate, cellular uptake, and bioavailability.

MATERIALS AND METHODS

Materials and Reagents. α-CD, γ-CD, TWEEN 80, and poloxamer 188 were purchased from J&K Scientific Co. Ltd., Beijing, China. HP-β-CD and β-CD were kindly provided as a gift sample from Roquette (China) Co. Ltd. Lutein was purchased from Speranza Co. Ltd., Shenzhen, China. All other reagents and solvents were of analytical grade.

Phase Solubility Study. The phase solubility investigation was carried out to determine the apparent stability constant (K), which represents the affinity of drug to the CDs in water.[33,34] The phase-solubility analyses were conducted by adding an excess amount of lutein to 3 mL of aqueous CD solutions with a series of increased concentrations of CDs from 0 to 50 mM, except β-CD with concentration range of 0 to 15 mM. The sealed glass containers were shaken at 37 °C for 48 h until equilibrium. Subsequently, samples were filtered through a 0.45 μm syringe filter. After that, the filtrate was analyzed on the Agilent 1200 HPLC system with DAD detector at 445 nm. An Eclipse XDB-C18 column (250 × 4.6 mm, 5 μm, Agilent, USA) with a guard column (Eclipse XDB-C18 column, 12.5 × 4.6 mm, 5 μm, Agilent, USA) was used, and samples were separated by a mobile phase consisting of methanol and acetonitrile (90:10, v/v) at a temperature of 20 °C and at a flow rate of 1.0 mL/min.

The apparent stability constant (K) of lutein−CD complexes with 1:1 stoichiometric ratio can be calculated using eq 1. The Gibbs free energy (ΔG) can be obtained by the $K_{1:1}$ value according to eq 2.

$$K_{1:1} = \frac{\text{slope}}{S_0(1 - \text{slope})} \quad (1)$$

The S_0 is the intrinsic solubility of lutein, and the slope is obtained using linear regression between the molar concentrations of lutein versus CDs in water.

$$\Delta G = -RT \ln K_{1:1} \quad (2)$$

R is the gas constant, and T is temperature in kelvins, while $K_{1:1}$ is the apparent stability constant of lutein−CD complexes with 1:1 stoichiometric ratio.

Screening of Optimal Lutein−CD-MCDS Formulation. Lutein−CD systems were screened for their solubility enhancement toward lutein in the presence and absence of auxiliary agents. The lutein−CD systems included lutein−CD binary systems, lutein−CD ternary systems and lutein−CD multiple-

DOI: 10.1021/acs.molpharmaceut.8b00056
Mol. Pharmaceutics 2018, 15, 1664−1673

component systems. For the binary systems, there existed only lutein and different CDs, and ternary systems had the added auxiliary agent of TWEEN 80, while multiple-component systems would add another auxiliary agent of poloxamer 188 on the base of ternary systems.

All systems were prepared by solvent evaporation method. Polymer carrier poloxamer 188 (100 mg) and the surfactant TWEEN 80 (100 μL) (if present) were first dissolved in ethanol to obtain a homogeneous solution. Then CDs (0.3 mmol) and lutein (10 mg) were added, followed by 5 mL of ethanol. The mixture was sonicated for about 30 min and then evaporated to dryness at 40 °C under vacuum in a rotary evaporator (EYELA OSB2100). The dried powders were pulverized, sifted, and stored in brown glass bottles for the following analysis. Samples in excess were added in 5 mL of water and then shaken on a shaker for 48 h at 37 °C. The resulting suspensions were filtered through a 0.45 μm syringe filter for HPLC analysis.

Physical mixtures were prepared at the same ratio as that in the optimal lutein−CD-MCDS formulation by uniformly mixing all the components in a sealed container. Samples were sieved through 80 mesh sieves and stored for further characterization.

Molecular Modeling of Lutein−CD Complexation and Lutein−CD-MCDS. *Molecular Structure Construction.* The molecular modeling studies of lutein−CDs and lutein−CD-MCDS were carried out using the AMBER14 and AMBERTOOL14 software package with Generalized Amber Force Field (GAFF) in the Antechamber module.[35]

Models of the molecular structures of three naturally occurring CDs (α-CD, β-CD, and γ-CD) were generated on the basis of crystallographic parameters provided by the Cambridge Crystallographic Data Centre (CCDC).[32] HP-β-CD was generated by manually attaching an isopropyl group on each 6-OH group of the glucopyranose by using Discovery Studio 4.5 Visualizer (DSV version 4.5). Lutein, TWEEN 80, and poloxamer 188 were drawn by DSV. The model of TWEEN 80 had an average degree of substitution ($x = y = z = w = 5$). The model of poloxamer 188 was composed of a central chain with 4 repeating units of propylene oxide, flanked by two chains with 12 repeating units of ethylene oxide (corresponding to around 15%).[36] The geometries of all structures were optimized using a fast, Dreiding-like force field.

Molecular Dynamic Simulation of Lutein−CD Complexation. The initial structures of supramolecular complexes were generated by docking lutein with different CDs (α-CD, β-CD, γ-CD, HP-β-CD) by the AutoDock Tools package and Autodock Vina.[37] Four stable binding structures from docking were loaded into the LEAP module with GAFF in the AmberTools 14 to build the initial structures of systems. Solvated systems were obtained by inserting the initial structures in the TIP3P water box with the 20 Å radius. The two-stage minimization procedures were adopted to allow the water box to relax and avoid the gaps between water and complexes. Steepest descent energy minimization for 5000 steps followed by 5000 steps of conjugate gradient minimization were performed under constant volume periodic boundaries by keeping the complexes fixed. Then the whole solvated systems were subjected to 20000 steps of energy minimization without any restraints. After the two-stage minimization, the solvated systems with a weak restraint on the complexes could be heated up from 0 to 310 K in 10000 steps by using the Langevin equilibration scheme to control the temperature. Finally, the whole solvated systems ran production simulations for 100 ns at the constant temperature of 310 K and the constant pressure of 1 bar. The time step was 2 fs, and nonbonded cutoff distance was 10 Å. During the simulations, the MD trajectory with coordinates, velocities, and energy was generated at every 10 ps. All the snapshot images were produced using VMD.[38]

Binding Affinity Calculation of Lutein−CD Complexation. The binding affinity "$\Delta G_{binding}$" was calculated using the MM-PBSA model, which calculated the free energy change upon the complex formation (ΔG_{com}) in comparison to individual potential energy (ΔG_{lutein}, ΔG_{CD}). The parameters, including electrostatic energy (ELE), van der Waals (VDW), hydrophobic contribution (PBSUR), and electrostatic contribution to the solvation free energy (PBCAL), were calculated for the complexes, lutein, and CDs.

$$\Delta G = \Delta G_{com} - \Delta G_{lutein} - \Delta G_{CD} \quad (3)$$

$$\Delta E = \Delta E_{ELE} + \Delta E_{VDW} + \Delta E_{PBSUR} + \Delta E_{PBCAL} \quad (4)$$

The binding entropy (ΔS) was calculated by normal-mode analysis using the ptraj program in AmberTools. The total entropy was contributed by the translational entropy, rotational entropy, and vibrational entropy. The binding free energy (ΔG) was calculated according to eq 5 by taking the entropy change into account.

$$\Delta G = \Delta E - T \cdot \Delta S \quad (5)$$

Molecular Dynamic Simulation of Lutein−CD-MCDS. All initial assemblies with lutein, CDs, and polymer molecules were constructed by using Packmol.[39] The number of drug and carrier molecules was calculated based on the molar concentration in the optimal lutein−CD-MCDS formulation. The simulated annealing method was used to mimic the preparation of lutein−CD-MCDS.[36] The minimization procedure was performed the same as in the above minimization stage of lutein−CD complexation simulation. During production simulation, the system was gradually heated from 0 K to 373 K in 5 ns, and then the temperature was kept constant for 5 ns. After melting procedure, the system was quickly cooled down from 373 to 273 K during 1 ns to solidify. Finally, the system was maintained at the temperature of 273 K for 14 ns to reach equilibration. All parameters (e.g., the temperature, pressure, and density) were controlled the same as above.

Physical Characterization of Lutein−CD-MCDS. *Dissolution Studies.* Dissolution studies were performed with a fully automated dissolution tester (Erweka DT700) with USP Paddle method under constant rotation speed of 100 rpm at 37 ± 0.5 °C. All tested samples containing 10 mg of pure lutein or its equivalents were placed in 900 mL of distilled water. 5 mL of sample was withdrawn at predetermined time intervals (5, 10, 15, 20, 30, 45, and 60 min). An equal volume of distilled water was added to maintain a constant volume of dissolution medium. Samples collected were filtered through a 0.45 μm syringe filter for HPLC analysis. All the dissolution tests were conducted in triplicate.

Differential Scanning Calorimetry (DSC). DSC analyses were conducted by using a DSC-60A to investigate the thermal characters of γ-CD, poloxamer 188, pure lutein, physical mixture, and lutein−CD-MCDS. All samples (~3 mg) were sealed in aluminum pans. Thermal analyses of samples were carried out at the heating rate of 10 °C·min^{-1} over the

DOI: 10.1021/acs.molpharmaceut.8b00056
Mol. Pharmaceutics 2018, 15, 1664−1673

temperature range of 30−210 °C under nitrogen gas. An empty aluminum pan was used as a reference.

Powder X-ray Diffraction (PXRD). The powder X-ray diffraction of samples was carried out on an in-house diffractometer (SmartLab9KW) employing the copper Kα_1 (λ = 1.54056 Å) and Kα_2 (λ = 1.54439 Å) with $I_{\alpha1}/I_{\alpha2}$ = 0.5 as the radiation with a 2θ step size of 0.004° at a voltage of 45 kV and a current of 200 mA and ambient conditions.

Fourier Transform Infrared Spectroscopy (FT-IR). FT-IR spectra were recorded by using a PerkinElmer Frontier. The samples were γ-CD, poloxamer 188, pure lutein, lutein−CD-MCDS, and physical mixture. Samples were milled with KBr to obtain fine powders and then compressed in press to obtain a thin tablet for analysis. Analyses were conducted with the scanning range of 400−4000 cm^{-1} at the resolution of 2 cm^{-1}. A blank KBr tablet was used as the reference.

Scanning Electron Microscopy (SEM). The ZEISS Sigma was used to evaluate the crystalline morphology of pure lutein, lutein−CD-MCDS, and physical mixtures. All samples were fixed on an aluminum stub and sputter-coated with gold. SEM study was performed under an accelerating voltage of 20 kV in vacuum and with 5000× magnification.

Cellular Uptake of Lutein in Caco-2 Cells. Caco-2 cells were seeded in 12-well plates at a density of 10^5 cells/well and incubated at 37 °C in an atmosphere of 5% CO_2 until they were about 80% confluence. The medium was changed every 2 days. Cell monolayers were used for the uptake studies and were treated with free lutein and lutein−CD-MCDS. The concentration of free lutein and lutein−CD-MCDS in the medium was 0.197 μg/mL, 25 μg/mL, and 50 μg/mL. Samples in serum-free Dulbecco's modification of Eagle's medium (DMEM) were added to the wells in triplicate and incubated for 24 h. After uptake by cells, the culture medium was removed and the cells were washed with cold PBS three times to remove all lutein on the surface of cell layers. The cells were lysed with trypsin and were centrifuged at 15000 rpm for 10 min at 4 °C. The supernatant was removed, and 500 μL of DMSO was added to the cells to dissolve the cellular lutein. The concentration of cellular lutein (μg/10^5 cells) was determined by using HPLC. The experiments were conducted in triplicate and were repeated thrice.

***In Vivo* Pharmacokinetic Study.** Eighteen male Sprague−Dawley (SD) rats with 300 ± 30 g weight were supplied by the Animal Center of University of Macau. They were housed in groups with no more than four per cage under standard conditions (controlled humidity, constant temperature at 22 °C, and 12 h dark−light cycle). They had free access to water and diet, and were permitted to acclimatize for 1 week. All the animal protocols and procedures were approved by Animal Ethical Committee at the Institute of Chinese Medical Sciences, University of Macau (Protocol ID: UMARE-017-2016) and were performed with the principles of the Guide for the Care and Use of Laboratory Animals.

Prior to the study, the rats were fasted for 12 h with free access to water and randomly assigned into three groups with 6 rats each. Each group was administered free lutein, commercial lutein soft capsules (lutein-SCs), and lutein−CD-MCDS, separately. Samples were delivered to rats in 1.0 mL of distilled water at the dose of 3 mg of lutein (about 10 mg/kg) via gastric gavage.[40] Blood samples were collected into heparin-coated tubes via the orbital sinus at the predetermined time intervals of 0.25, 0.5, 1, 1.5, 2, 3, 4, 6, 8, and 10 h after gastric gavage. All collected samples were centrifuged at 3000 rev/min for 10 min to obtain plasma samples and then were stored at −80 °C for further analysis.

Lutein in the plasma was extracted according to a previous publication.[41] Briefly, 10 μL of internal standard α-tocopherol (300 μg/mL) was added into 100 μL of thawed plasma samples. The mixed samples were extracted sequentially with 300 μL of dichloromethane−methanol (1:2, v/v). After vortex mixing, 200 μL of hexane was added, mixed, and then centrifuged at 4000 rpm for 10 min. 200 μL of the resultant upper solution was collected, and the extraction procedure was repeated for the lower mixtures. Then the clear supernatant was evaporated in a centrifugal vacuum evaporator at 35 °C. The residue was redissolved in 100 μL of mobile phase and was used for HPLC analysis. The analytical conditions were the same as those for the above HPLC protocol. Lutein and α-tocopherol were monitored at wavelengths of 450 and 294 nm, respectively. Their concentrations were calculated using standard curves constructed with authenticated standards. Pharmacokinetic parameters, such as C_{max}, T_{max}, and AUC, were calculated by the pharmacokinetic program of DAS 2.0.

RESULTS AND DISCUSSION

Phase Solubility Study. Phase solubility curves of lutein with different CDs are shown in Figure 2, whereas, K_c, R^2, and

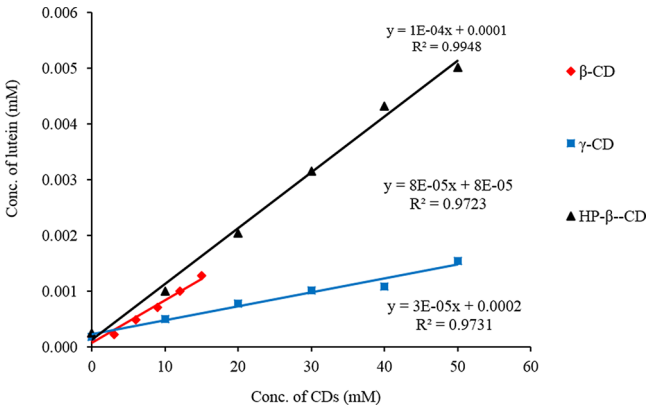

Figure 2. Phase solubility curves of lutein with different CDs in distilled water at 37 ± 0.5 °C.

Table 1. Phase Solubility Study of Lutein with Different CDs in Distilled Water at 37 ± 0.5 °C

system	K_c (M^{-1})[a]	R^2[b]	ΔG^c (kJ mol^{-1})
lutein−γ-CD	93.170	0.973	−11.692
lutein−β-CD	248.467	0.972	−14.221
lutein−HP-β-CD	310.590	0.995	−14.797

[a] K_c (M^{-1}) indicates stability constant. [b] R^2, correlation coefficient. [c] ΔG (kJ mol^{-1}), Gibbs free energy at the temperature of 37 ± 0.5 °C.

ΔG values are presented in Table 1. The solubility of lutein increased linearly with respect to the concentration of γ-CD, β-CD, and HP-β-CD, which indicated a typical A_L type diagram. The A_L type and slope values of the curves less than unity suggested the 1:1 stoichiometry between γ-CD, β-CD, and HP-β-CD. The correlation between the solubility of lutein and concentration of α-CD was not linear, but a fluctuating trend (not shown in Figure 2).

DOI: 10.1021/acs.molpharmaceut.8b00056
Mol. Pharmaceutics 2018, 15, 1664−1673

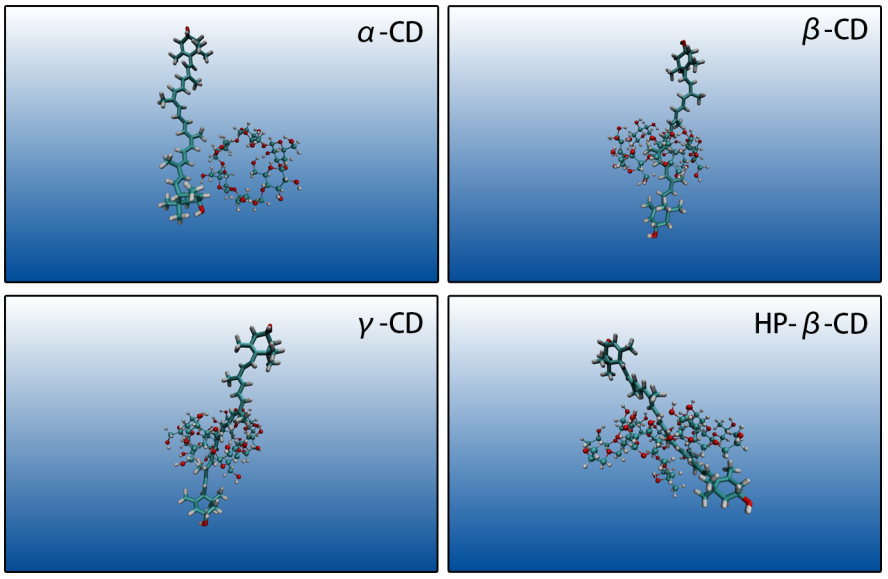

Figure 3. Snapshots of binding pose of lutein−CDs at 100 ns. Carbon elements are indicated in blue bonds, hydrogen elements in white, and oxygen elements in red.

Table 2. Binding Free Energy of Lutein−CD Complexation by the MM-PBSA Method

	ELE[a]	VDW[b]	PBSUR[c]	PBCAL[d]	PBTOT[e] (kcal/mol)	$T\Delta S$[f] (kcal/mol)	ΔG (kcal/mol)	ΔG (kJ/mol)
β-CD	−2.18	−25.44	−2.71	13.20	−17.12	−14.46	−2.66	−11.13
γ-CD	−4.20	−35.22	−3.64	23.83	−19.45	−17.76	−1.69	−7.07
HP-β-CD	−2.61	−30.63	−3.12	17.55	−18.81	−15.68	−3.13	−13.10

[a]ELE, electrostatic energy as calculated by the MM force field. [b]VDW, van der Waals contribution from MM. [c]PBSUR, hydrophobic contribution to the solvation free energy calculated by an empirical model. [d]PBCAL, the electrostatic contribution to the solvation free energy. [e]PBTOT, final estimated binding free energy. $T\Delta S$. [f]Total entropy.

The calculated stability constants showed an order of HP-β-CD (310.590 M^{-1}) > β-CD (248.467 M^{-1}) > γ-CD (93.170 M^{-1}). The higher K_c suggested more stable complex formation with improved complexation of CDs with lutein. As shown in Table 1, the negative ΔG in the complexation of lutein with these three CDs in water revealed a spontaneous and exothermic process. Although the water-soluble complexes were formed, the low values of stability constants and Gibbs free energy suggested the very weak interaction between CDs and lutein.

Investigation of Molecular Mechanism of Lutein−CD Complexation by MD Simulation. To further investigate the molecular interaction between lutein and CDs, molecular dynamic simulations of lutein−CD complexation in water were conducted. Snapshots of binding pose of lutein with four CDs after 100 ns simulation are shown in Figure 3. From the snapshot of lutein with α-CD, the complexation of lutein and α-CD was found to be unstable because the lutein molecule cannot bind with the α-CD molecule. This may be because the small α-CD ring cannot host the relatively big lutein molecule.

Another three CDs presented similarly stable binding pose with 1:1 inclusion complexes. One hexatomic ring of lutein molecule inserted through the 2-OH and 3-OH group of glucopyranose and finally oriented toward the 6-OH group of glucopyranose. Compared to the other end of lutein, the inserted ring was more closely associated with the CD cavity. As shown in Figure 3, both hexatomic rings of lutein were outside the hydrophobic CD inner cavity, while two or three conjugated double bonds were positioned inside the cavity. The binding poses exhibited the combination of electrostatic and hydrophobic nonbonded interactions between lutein and CD molecules. However, γ-CD with the largest diameter was flexible to accommodate the lutein molecule, which may lead to weak interaction with lutein. The substituted isopropyl groups on the 6-OH group of HP-β-CD spatially hindered the move of lutein molecule, which may result in the highest binding energy.

Table 2 shows the binding free energy of lutein−CD complexation by the MM-PBSA approach. For the lutein−CD complexation, the van der Waals force was the highest contribution compared to the electrostatic interaction and hydrophobic contribution. The negative ΔS value for these three kinds of lutein−CDs revealed the formation of complexes, because lutein was trapped and had a limited mobility. The negative Gibbs binding free energy suggested that lutein−CD complexation in pure water was a favorable, spontaneous, and exothermic process. For these three CDs (listed in Table 2), the lutein exhibited the highest binding affinity (−13.10 kJ/mol) with HP-β-CD, followed by β-CD and γ-CD. The trend of Gibbs binding free energy calculated by MD simulation was in line with the experimental results of phase solubility study. For the system of lutein and α-CD (calculated, but not shown in the table), both binding free energy and entropy were positive, which also revealed that no inclusion complex formed.

Screening of Optimal Lutein−CD-MCDS. Lutein exhibited very low saturation solubility in distilled water (0.197 ± 0.013 μg/mL). Although lutein could form complexes with the three kinds of CDs, the CD complexation had very limited effects on the improvements of lutein solubility, which are depicted in Figure 4. The lutein−CD binary systems shown the

DOI: 10.1021/acs.molpharmaceut.8b00056
Mol. Pharmaceutics 2018, 15, 1664−1673

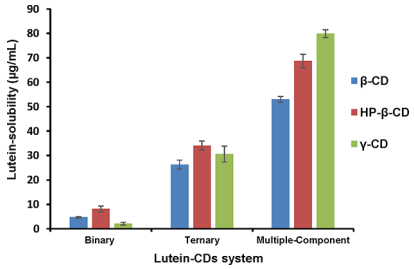

Figure 4. Lutein saturation solubility of different lutein−CD systems in distilled water. Binary systems consisted of lutein (10 mg) and CDs (0.3 mmol), and ternary systems had the added auxiliary agent of TWEEN 80 (100 μL). Multiple-component systems were composed of lutein (10 mg), CDs (0.3 mmol), TWEEN 80 (100 μL), and poloxamer 188 (100 mg).

lowest solubility with no more than 10 μg/mL. Auxiliary substances are known to interact with the outer surface of CD or drug−CD complex, forming aggregates to improve stability constants (K_c) and complexation efficiency (CE) . The lutein−CD ternary systems with the added TWEEN 80 had an improvement in lutein's solublity compared to binary systems, especially for the γ-CD system. Furthermore, the lutein solubility in lutein−CD-MCDS with γ-CD, β-CD, and HP-β-CD was found to be 79.94 ± 2.21 μg/mL, 52.97 ± 2.53 μg/mL, and 68.71 ± 3.96 μg/mL, which increased approximately to 406-fold, 270-fold, and 350-fold that of pure lutein, respectively. As depicted in Figure 4, it was found that, among these lutein−CD systems, the highest solubility of lutein was observed in the lutein−γ-CD multiple-component system. Therefore, the lutein−γ-CD-MCDS was regarded as the optimal formulation for the improvement of lutein solubility.

Investigation of Molecular Mechanism of Lutein−CD-MCDS by MD Simulation. MD simulation was conducted to provide better understanding of molecular interactions between lutein and carriers in the systems. The initial structure of lutein−CD-MCDS (shown in Figure 5A) was packed by the program of Packmol. The packing optimized the construction way of molecules and guaranteed short-range repulsive interactions not to disrupt simulation. Lutein did not insert into the inner cavity of γ-CD: it hung over one of the γ-CD rings and was surrounded by five γ-CD rings, while one of the linear poloxamer 188 polymer chains passed through the γ-CD ring. The optimization of initial structure suggested that the polymer chains of carriers in the multiple-component systems would compete for γ-CD rings. However, the competition could be conducive to improving the stability of the entire system. After a simulated annealing procedure of 25 ns simulation, the entire system reached equilibrium and stability. Lutein molecule inserted into one of the γ-CD rings to form an inclusion complex like that in the lutein−CD binary system. The two hexatomic rings and remaining conjugated double bonds were also covered by other γ-CD molecules. Linear TWEEN 80 and poloxamer 188 polymer chains started to bend and introduced bridging interaction between lutein and γ-CDs to increase the stability of the complex by occupying the outer surface of the inclusion complex. Therefore, TWEEN 80 and poloxamer 188 formed the aggregates to increase the solubility by increasing the hydrophilic surface of the supramolecular inclusion complex. Furthermore, γ-CD also presented self-assembled aggregates with the orientation of head-to-head and tail-to-head. Actually, CDs, especially γ-CD, were able to self-assemble to form nanosized aggregates for the CD solubilization of poorly soluble drugs.[42]

Characterization of Lutein−CD-MCDS. *Dissolution Studies.* The *in vitro* dissolution studies were performed to investigate the enhanced release behavior of lutein−CD-MCDS, as shown in Figure 6. The dissolution study showed

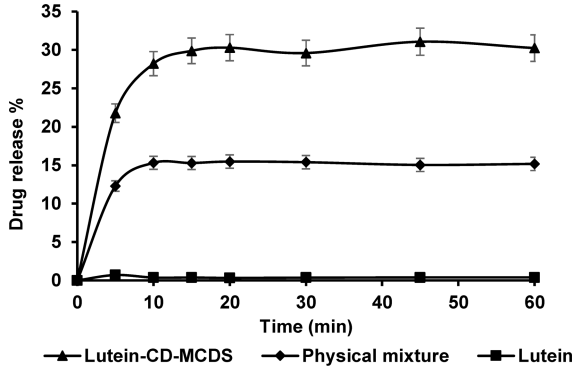

Figure 6. Dissolution profiles of lutein−CD-MCDS, physical mixture, and pure lutein.

less than 2% release of pure lutein powder within 60 min because of the low solubility of lutein in distilled water. The higher drug release from physical mixture than that of pure lutein could be attributed to formation of *in situ* soluble complex with γ-CD in the dissolution medium, or it could be

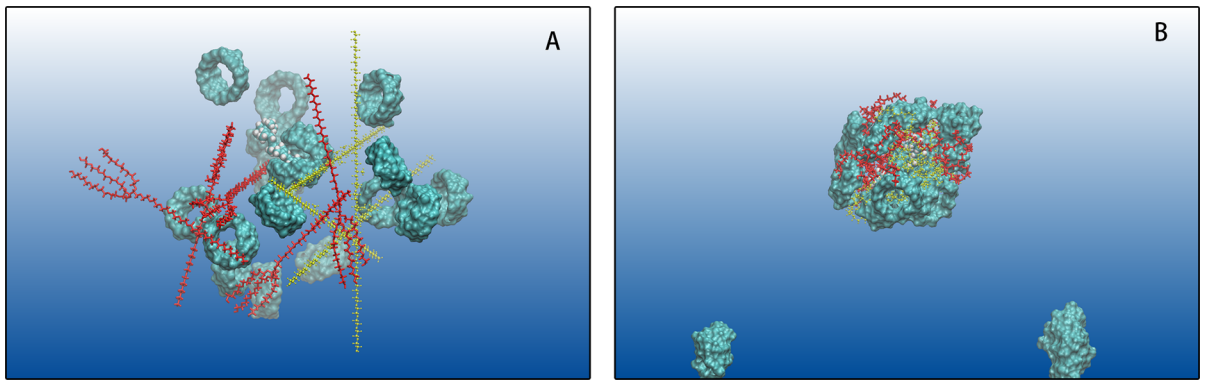

Figure 5. Snapshots of the initial frame (A) after packing by Packmol and final frame (B) (at 25 ns) for the molecular dynamic simulations of lutein−CD-MCDS. Lutein molecules are indicated in spherical structure, poloxamer 188 in yellow, TWEEN 80 in red, and γ-CD in blue.

DOI: 10.1021/acs.molpharmaceut.8b00056
Mol. Pharmaceutics 2018, 15, 1664−1673

that the auxiliary substance like poloxamer 188 and TWEEN 80 increased the aqueous solubility of drug by improving the wettability of lutein. Lutein−CD-MCDS clearly showed a significant improvement in the dissolution rate. The lutein−CD-MCDS showed 2-fold and 10-fold increase in drug release than physical mixture and pure lutein, respectively. Our formulation not only increased the lutein solubility but also played an important role in inhibiting crystallization and precipitation of lutein in the dissolution process.

Differential Scanning Calorimetry (DSC). The DSC curves of different samples are presented in Figure 7. Clearly, a single endothermic peak of pure lutein was observed at 162.51 °C, which indicated the intrinsic melting points of lutein (Figure 7C). Poloxamer 188 showed a sharp endothermic peak at 49.24 °C for its crystalline nature (Figure 7D). The γ-CD thermogram exhibited a broad endothermic peak in the range of 60−100 °C, which may be attributable to the dehydration process (Figure 7E). Furthermore, the lutein melting peak in the physical mixture shifted to a relatively lower temperature of 142.46 °C and the peak intensity of poloxamer 188 was reduced (Figure 7B). These observed peak shifts of physical mixture may be caused by the interactions between lutein and carriers, but not formation of true complexes. The disappearance of lutein melting peak in lutein−CD-MCDS indicated that lutein existed in the amorphous state rather than a crystalline form (Figure 7A).

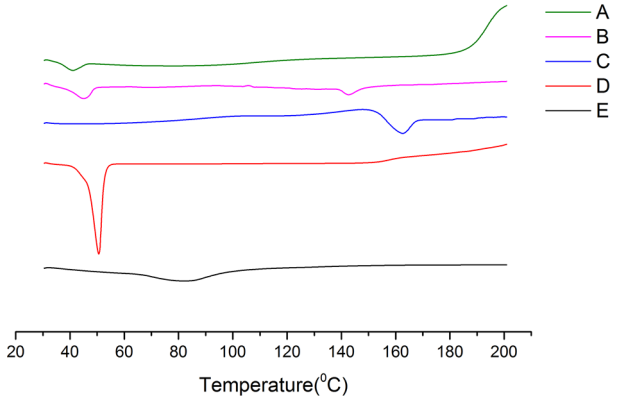

Figure 7. DSC thermograms for (A) lutein−CD-MCDS, (B) physical mixture, (C) pure lutein, (D) poloxamer 188, and (E) γ-CD.

Powder X-ray Diffraction (PXRD). The PXRD diffractograms of pure lutein, γ-CD, poloxamer 188, physical mixture, and lutein−CD-MCDS are shown in Figure 8. Poloxamer 188 showed highly crystalline nature with two characteristic peaks at 19.18° and 23.34° (Figure 8D). γ-CD also exhibited a typical crystalline diffraction pattern with major peaks between 10° and 25° (Figure 8E), while the characteristic peaks of lutein were relatively weak but still could be identified. Three major peaks at the 2θ values of 8.24°, 14.04°, and 20.44° indicated the crystalline structure of lutein (Figure 8C). Two of the characteristic crystalline peaks of lutein at 8.24° and 14.04° were also observed in the physical mixture, which indicated that the good crystalline form of lutein still existed in the physical mixture (Figure 8B). In contrast, the disappearance of characteristic peaks of lutein in lutein−CD-MCDS suggested that the crystalline lutein may change into an amorphous state or be molecularly dispersed in the lutein−CD-MCDS (Figure 8A).

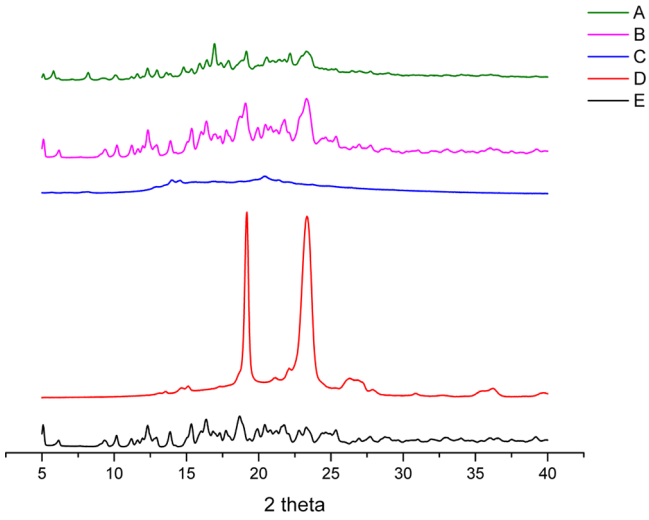

Figure 8. PXRD diagrams of (A) lutein−CD-MCDS, (B) physical mixture, (C) pure lutein, (D) poloxamer 188, and (E) γ-CD.

Fourier Transform Infrared Spectroscopy (FT-IR). Figure 9 shows the IR spectra of pure lutein, TWEEN 80, γ-CD, poloxamer 188, physical mixture, and lutein−CD-MCDS at 400−4000 cm^{-1}. The characteristic absorption peaks of lutein appeared at 2922 and 2850 cm^{-1} denoting asymmetric and symmetric stretching vibrations of CH_2 and CH_3, 1450 cm^{-1} for CH_2 scissoring, and 1365 cm^{-1} for splitting due to dimethyl group. Lutein powder also had a peak at 966 cm^{-1} due to trans-conjugated alkene −CH═CH− out of plane deformation mode (Figure 9C). However, the intensity of the characteristic bands of lutein in the lutein−CD-MCDS spectra was strongly reduced. The typical peak at 966 cm^{-1} was found to completely disappear. Another prominent peak at 2922 cm^{-1} became flat in the lutein−CD-MCDS (Figure 9A). Compared with the physical mixture, some typical peaks of lutein in lutein−CD-MCDS also showed slight broadening, flattening, change, or disappearing, which were indicative of new molecular interactions or a new solid system. Although FT-IR spectros-

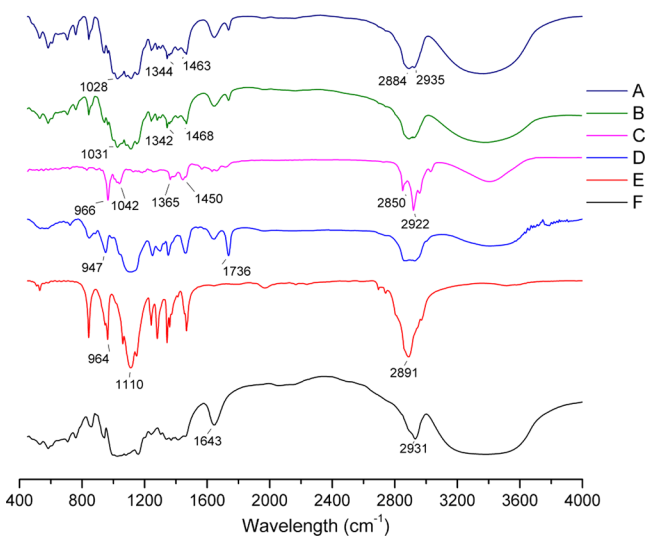

Figure 9. FT-IR spectra of (A) lutein−CD-MCDS, (B) physical mixture, (C) pure lutein, (D) TWEEN 80, (E) poloxamer 188, and (F) γ-CD.

DOI: 10.1021/acs.molpharmaceut.8b00056
Mol. Pharmaceutics 2018, 15, 1664−1673

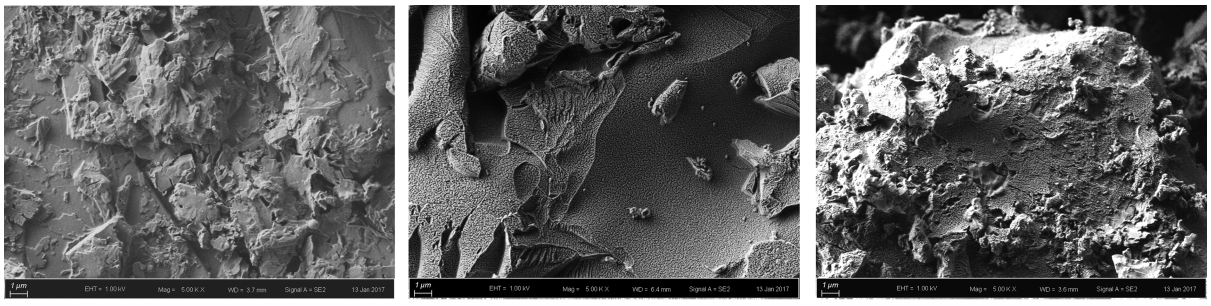

Figure 10. Scanning electronic microscopy images of (A) pure lutein, (B) lutein−CD-MCDS, and (C) physical mixtures. Scale bar represents 1.0 μm, and magnification is 5000×.

copy can detect the structural changes or lack of a crystal structure by the changes of the molecular bonding energy between functional groups, not all peaks in the IR spectrum are sensitive to crystalline changes.[43] In addition, the characteristic absorption peaks of different components may interfere with each other or overshadow the peak shifts, especially for such a complex system. The molecular interaction predicted by the computational modeling was in agreement with the observed IR spectral changes. The trans-conjugated alkene −CH═CH− of lutein in the aggregates was wrapped by other carriers in the molecular simulation, which was also evident in the IR spectra.

Scanning Electron Microscopy (SEM). SEM images of pure lutein, lutein−CD-MCDS, and physical mixtures are shown in Figure 10. Pure lutein was an irregular-shaped crystal with fractured edges (Figure 10A). SEM analysis demonstrated higher degree of drug dispersion and completely homogeneous system in lutein−CD-MCDS, in comparison with the physical mixture, which showed a simple combination of lutein and carriers (Figure 10B,C). The original morphological features of lutein have changed in lutein−CD-MCDS, which indicates the formation of a new lutein-carrier compound and may be related to the improvement of the dissolution rate of lutein.

Cell Uptake of Lutein. In the cellular uptake experiment, Caco-2 cells were treated with pure lutein at 0.197 μg/mL and lutein−CD-MCDS at 25 μg/mL and 50 μg/mL, respectively. As shown in Figure 11, the cellular accumulations of lutein from pure lutein solution after 12 h incubation were very low at 0.005 μg/cm^2. For lutein−CD-MCDS at 25 μg/mL and 50 μg/mL, the apparent cellular uptakes were 0.257 μg/mL and 0.348 μg/mL, respectively. The lutein cellular uptake of lutein−CD-MCDS was about 50- and 70-fold higher than that of pure lutein.

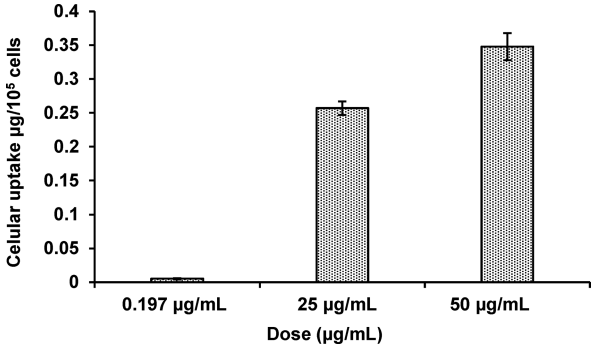

Figure 11. Lutein absorption in differentiated Caco-2 cells treated with pure lutein at 0.197 μg/mL, lutein−CD-MCDS at 25 μg/mL, and lutein−CD-MCDS at 50 μg/mL. Values are represented as mean ± SD (n = 3).

***In Vivo* Pharmacokinetic Study.** Although the prepared lutein−CD-MCDS showed high dissolution rate and cellular uptake, it still needed to be further evaluated for its *in vivo* bioavailability. In the pharmacokinetic study, rats were orally administered 10 mg/kg body weight of pure lutein, lutein−CD-MCDS, and marketed lutein-SCs. The blood was collected at 0.25, 0.5, 1, 1.5, 2, 3, 4, 6, 8, and 10 h. The drug plasma concentration−time profiles of three samples are shown in Figure 12, and the main pharmacokinetic parameters are listed in Table 3. Obviously, both lutein−CD-MCDS and marketed lutein-SCs showed a remarkably higher C_{max} and area-under-the-curve (AUC_{0-t}) than pure lutein. The C_{max} of lutein−CD-MCDS was 135.8 ng·mL^{-1}, which was 6.7-fold and 1.1-fold greater than that of pure lutein and marketed lutein-SCs, respectively. The area-under-the-curve (AUC_{0-t}) of lutein−CD-MCDS was 633.0 ng·h·mL^{-1}, compared with 539.5 ng·h·

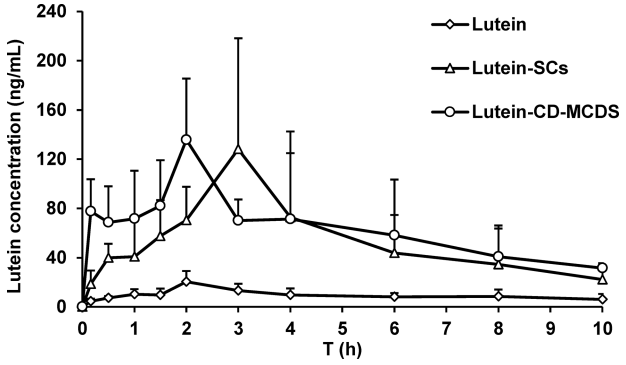

Figure 12. Mean plasma concentration−time curves of pure lutein, lutein−CD-MCDS, and marketed lutein-SCs after oral administration of 10 mg/kg BW in rats (mean ± SD, n = 6).

Table 3. Pharmacokinetic Parameters of Pure Lutein, Lutein−CD-MCDS, and Marketed Lutein-SCs after Oral Administration of 10 mg/kg BW in Rats

parameters	pure lutein	lutein−CD-MCDS	lutein-SCs
T_{max} (h)	2	2	3
C_{max} (ng·mL^{-1})	20.4 ± 8.6	135.8 ± 49.7	128.1 ± 90.1
AUC_{0-10} (ng·h·mL^{-1})	95.7 ± 32.6	633.0 ± 209.7	539.5 ± 298.9
$AUC_{0-\infty}$ (ng·h·mL^{-1})	173.5 ± 29.3	861.5 ± 215.4	655.7 ± 303.9

DOI: 10.1021/acs.molpharmaceut.8b00056
Mol. Pharmaceutics 2018, 15, 1664−1673

mL^{-1} for the commercial lutein-SCs and 95.7 $ng \cdot h \cdot mL^{-1}$ for pure lutein. Hence, the relative bioavailability of lutein−CD-MCDS and lutein-SCs reference was 661.2% and 563.5% in comparison with pure lutein, respectively. The better absorption of commercial lutein-SCs was mostly due to adding high fat components in the soft capsule, as the oil components could enhance lutein absorption in the small intestine. However, a small amount of oil component in lutein-SCs may have less effect on the lutein absorption in the human body because of much larger gastrointestinal volume than that of rats. Further, the C_{max} and AUC for the lutein−CD-MCDS were 6.7-fold and 6.6-fold greater than those of free lutein, which clearly indicated that the developed lutein−CD-MCDS successfully improved the lutein *in vivo* absorption.

■ CONCLUSION

The present study successfully developed a highly soluble lutein−CD multiple-component delivery system to enhance its solubility, dissolution rate, and bioavailability by combined modeling and experimental methods. Molecular dynamics simulation provided clear molecular mechanism of the formulations. Different experimental approaches (e.g., DSC, FT-IR, SEM, and PXRD) indicated that the crystalline nature of lutein was changed to an amorphous nature in the formulation. The optimal lutein−CD multiple-component delivery system did improve the cell uptake and bioavailability of lutein. Current research demonstrated that molecular modeling is a useful tool of formulation screening for better medicine.

■ AUTHOR INFORMATION

Corresponding Author

*Institute of Chinese Medical Sciences (ICMS), University of Macau, Avenida da Universidade, Taipa, Macau. Tel: (853) 8822 4514. E-mail: defangouyang@umac.mo.

ORCID

Qianqian Zhao: 0000-0002-6647-3762

Ru Yan: 0000-0001-6268-360X

Dongsheng Cao: 0000-0003-3604-3785

Notes

The authors declare no competing financial interest.

■ ACKNOWLEDGMENTS

Work presented in this article was supported by the FDCT Project 009/2015/A and the University of Macau Research Grants (MYRG2016-00038-ICMS-QRCM and MYRG2016-00040-ICMS-QRCM).

■ REFERENCES

(1) Ku, M. S.; Dulin, W. A biopharmaceutical classification-based Right-First-Time formulation approach to reduce human pharmacokinetic variability and project cycle time from First-In-Human to clinical Proof-Of-Concept. *Pharm. Dev. Technol.* **2012**, *17* (3), 285−302.

(2) Shanmugam, S.; Park, J.-H.; Kim, K. S.; Piao, Z. Z.; Yong, C. S.; Choi, H.-G.; Woo, J. S. Enhanced bioavailability and retinal accumulation of lutein from self-emulsifying phospholipid suspension (SEPS). *Int. J. Pharm.* **2011**, *412* (1), 99−105.

(3) Chatterjee, M.; Roy, K.; Janarthan, M.; Das, S.; Chatterjee, M. Biological activity of carotenoids: its implications in cancer risk and prevention. *Curr. Pharm. Biotechnol.* **2012**, *13* (1), 180−190.

(4) Bone, R. A.; Landrum, J. T.; Mayne, S. T.; Gomez, C. M.; Tibor, S. E.; Twaroska, E. E. Macular pigment in donor eyes with and without AMD: a case-control study. *Invest. Ophthalmol. Vis. Sci.* **2001**, *42* (1), 235−240.

(5) Beatty, S.; Murray, I. J.; Henson, D. B.; Carden, D.; Koh, H.-H.; Boulton, M. E. Macular pigment and risk for age-related macular degeneration in subjects from a Northern European population. *Invest. Ophthalmol. Vis. Sci.* **2001**, *42* (2), 439−446.

(6) Chung, H.-Y.; Rasmussen, H. M.; Johnson, E. J. Lutein bioavailability is higher from lutein-enriched eggs than from supplements and spinach in men. *J. Nutr.* **2004**, *134* (8), 1887−1893.

(7) Sato, Y.; Kobayashi, M.; Itagaki, S.; Hirano, T.; Noda, T.; Mizuno, S.; Sugawara, M.; Iseki, K. Protective effect of lutein after ischemia-reperfusion in the small intestine. *Food Chem.* **2011**, *127* (3), 893−898.

(8) Kotake-Nara, E.; Nagao, A. Absorption and metabolism of xanthophylls. *Mar. Drugs* **2011**, *9* (6), 1024−1037.

(9) Mitri, K.; Shegokar, R.; Gohla, S.; Anselmi, C.; Müller, R. H. Lipid nanocarriers for dermal delivery of lutein: preparation, characterization, stability and performance. *Int. J. Pharm.* **2011**, *414* (1), 267−275.

(10) Pintea, A.; Diehl, H. A.; Momeu, C.; Aberle, L.; Socaciu, C. Incorporation of carotenoid esters into liposomes. *Biophys. Chem.* **2005**, *118* (1), 7−14.

(11) Mamatha, B. S.; Baskaran, V. Effect of micellar lipids, dietary fiber and β-carotene on lutein bioavailability in aged rats with lutein deficiency. *Nutrition* **2011**, *27* (9), 960−966.

(12) Shanmugam, S.; Baskaran, R.; Balakrishnan, P.; Thapa, P.; Yong, C. S.; Yoo, B. K. Solid self-nanoemulsifying drug delivery system (S-SNEDDS) containing phosphatidylcholine for enhanced bioavailability of highly lipophilic bioactive carotenoid lutein. *Eur. J. Pharm. Biopharm.* **2011**, *79* (2), 250−257.

(13) Murillo, A. G.; Aguilar, D.; Norris, G. H.; DiMarco, D. M.; Missimer, A.; Hu, S.; Smyth, J. A.; Gannon, S.; Blesso, C. N.; Luo, Y.; Fernandez, M. L. Compared with Powdered Lutein, a Lutein Nanoemulsion Increases Plasma and Liver Lutein, Protects against Hepatic Steatosis, and Affects Lipoprotein Metabolism in Guinea Pigs. *J. Nutr.* **2016**, *146* (10), 1961−1969.

(14) Frede, K.; Henze, A.; Khalil, M.; Baldermann, S.; Schweigert, F. J.; Rawel, H. Stability and cellular uptake of lutein-loaded emulsions. *J. Funct. Foods* **2014**, *8*, 118−127.

(15) Uekama, K.; Hirayama, F.; Irie, T. Cyclodextrin drug carrier systems. *Chem. Rev.* **1998**, *98* (5), 2045−2076.

(16) Loftsson, T.; Brewster, M. E. Pharmaceutical applications of cyclodextrins: basic science and product development. *J. Pharm. Pharmacol.* **2010**, *62* (11), 1607−1621.

(17) Kurkov, S. V.; Loftsson, T. Cyclodextrins. *Int. J. Pharm.* **2013**, *453* (1), 167−180.

(18) Zhao, Q.; Zhang, W.; Wang, R.; Wang, Y.; Ouyang, D. Research Advances in Molecular Modeling in Cyclodextrins. *Curr. Pharm. Des.* **2017**, *23* (3), 522−531.

(19) Nalawade, P.; Gajjar, A. Preparation and characterization of spray dried complexes of lutein with cyclodextrins. *J. Inclusion Phenom. Macrocyclic Chem.* **2015**, *83* (1−2), 77−87.

(20) Liu, C. H.; Chiu, H. C.; Wu, W. C.; Sahoo, S. L.; Hsu, C. Y. Novel Lutein Loaded Lipid Nanoparticles on Porcine Corneal Distribution. *J. Ophthalmol.* **2014**, *2014*, 304694.

(21) Prochowicz, D.; Kornowicz, A.; Justyniak, I.; Lewiński, J. Metal complexes based on native cyclodextrins: Synthesis and structural diversity. *Coord. Chem. Rev.* **2016**, *306*, 331−345.

(22) Zhu, Q.; Guo, T.; Xia, D.; Li, X.; Zhu, C.; Li, H.; Ouyang, D.; Zhang, J.; Gan, Y. Pluronic F127-modified liposome-containing tacrolimus−cyclodextrin inclusion complexes: improved solubility, cellular uptake and intestinal penetration. *J. Pharm. Pharmacol.* **2013**, *65* (8), 1107−1117.

(23) Szente, L.; Szejtli, J.; Kis, G. L. Spontaneous opalescence of aqueous γ-Cyclodextrin solutions: Complex formation or self-aggregation? *J. Pharm. Sci.* **1998**, *87* (6), 778−781.

(24) Thakur, S. S.; Parekh, H. S.; Schwable, C. H.; Gan, Y.; Ouyang, D. Solubilization of Poorly Soluble Drugs: Cyclodextrin-Based Formulations. In *Computational Pharmaceutics: Application of Molec-*

DOI: 10.1021/acs.molpharmaceut.8b00056
Mol. Pharmaceutics 2018, 15, 1664−1673

ular Modeling in Drug Delivery; Ouyang, D., Smith, S. C., Eds.; Wiley: 2015; pp 31−51, DOI: 10.1002/9781118573983.ch3.
(25) Chen, W.; Gu, B.; Wang, H.; Pan, J.; Lu, W.; Hou, H. Development and evaluation of novel itraconazole-loaded intravenous nanoparticles. *Int. J. Pharm.* **2008**, *362* (1), 133−140.
(26) Sherje, A. P.; Kulkarni, V.; Murahari, M.; Nayak, U. Y.; Bhat, P.; Suvarna, V.; Dravyakar, B. Inclusion Complexation of Etodolac with Hydroxypropyl-beta-cyclodextrin and Auxiliary Agents: Formulation Characterization and Molecular Modeling Studies. *Mol. Pharmaceutics* **2017**, *14* (4), 1231−1242.
(27) Veiga, M. D.; Ahsan, F. Influence of surfactants (present in the dissolution media) on the release behaviour of tolbutamide from its inclusion complex with β-cyclodextrin. *Eur. J. Pharm. Sci.* **2000**, *9* (3), 291−299.
(28) Raffaini, G.; Ganazzoli, F.; Malpezzi, L.; Fuganti, C.; Fronza, G.; Panzeri, W.; Mele, A. Validating a strategy for molecular dynamics simulations of cyclodextrin inclusion complexes through single-crystal X-ray and NMR experimental data: a case study. *J. Phys. Chem. B* **2009**, *113* (27), 9110−9122.
(29) Leach, A. R. *Molecular modelling: principles and applications*; Pearson Education: 2001.
(30) Jullian, C.; Miranda, S.; Zapata-Torres, G.; Mendizábal, F.; Olea-Azar, C. Studies of inclusion complexes of natural and modified cyclodextrin with (+) catechin by NMR and molecular modeling. *Bioorg. Med. Chem.* **2007**, *15* (9), 3217−3224.
(31) Zheng, Y.; Haworth, I. S.; Zuo, Z.; Chow, M. S.; Chow, A. H. Physicochemical and structural characterization of Quercetin-β-Cyclodextrin Complexes. *J. Pharm. Sci.* **2005**, *94* (5), 1079−1089.
(32) Wang, R.; Zhou, H.; Siu, S. W.; Gan, Y.; Wang, Y.; Ouyang, D. Comparison of three molecular simulation approaches for cyclodextrin-ibuprofen complexation. *J. Nanomater.* **2015**, *16* (1), 267.
(33) Higuchi, T.; Connors, K. Phase-solubility Techniques. *Adv. Anal. Chem. Instr.* **1965**, *4*, 117−212.
(34) Loftsson, T.; Hreinsdóttir, D.; Másson, M. Evaluation of cyclodextrin solubilization of drugs. *Int. J. Pharm.* **2005**, *302* (1), 18−28.
(35) Wang, J.; Wolf, R. M.; Caldwell, J. W.; Kollman, P. A.; Case, D. A. Development and testing of a general amber force field. *J. Comput. Chem.* **2004**, *25* (9), 1157−1174.
(36) Ouyang, D. Investigating the molecular structures of solid dispersions by the simulated annealing method. *Chem. Phys. Lett.* **2012**, *554*, 177−184.
(37) Trott, O.; Olson, A. J. AutoDock Vina: improving the speed and accuracy of docking with a new scoring function, efficient optimization, and multithreading. *J. Comput. Chem.* **2010**, *31* (2), 455−461.
(38) Humphrey, W.; Dalke, A.; Schulten, K. VMD: visual molecular dynamics. *J. Mol. Graphics* **1996**, *14* (1), 33−38.
(39) Martínez, L.; Andrade, R.; Birgin, E. G.; Martínez, J. M. PACKMOL: a package for building initial configurations for molecular dynamics simulations. *J. Comput. Chem.* **2009**, *30* (13), 2157−2164.
(40) Kamil, A.; Smith, D. E.; Blumberg, J. B.; Astete, C.; Sabliov, C.; Chen, C.-Y. O. Bioavailability and biodistribution of nanodelivered lutein. *Food Chem.* **2016**, *192*, 915−923.
(41) Sugawara, T.; Kushiro, M.; Zhang, H.; Nara, E.; Ono, H.; Nagao, A. Lysophosphatidylcholine enhances carotenoid uptake from mixed micelles by Caco-2 human intestinal cells. *J. Nutr.* **2001**, *131* (11), 2921−2927.
(42) Messner, M.; Kurkov, S. V.; Jansook, P.; Loftsson, T. Self-assembled cyclodextrin aggregates and nanoparticles. *Int. J. Pharm.* **2010**, *387* (1), 199−208.
(43) Leuner, C.; Dressman, J. Improving drug solubility for oral delivery using solid dispersions. *Eur. J. Pharm. Biopharm.* **2000**, *50* (1), 47−60.

DOI: 10.1021/acs.molpharmaceut.8b00056
Mol. Pharmaceutics 2018, 15, 1664−1673